Assessment of Steel Reinforcement Corrosion Resistance in Sulphur Infiltrated Concrete: An Electrochemical and Compositional Analysis

Gayatri Pathak
Amity School of Engineering and Technology, Amity University Maharashtra, Mumbai, India
gayatrid676@gmail.com (corresponding author)

S.Sangita Mishra
Amity School of Engineering and Technology, Amity University Maharashtra, Mumbai, India
ssmishra@mum.amity.edu

Shrikant Charhate
NICMAR University of Construction Studies, Hyderabad, India
shrikant.charhate@hyd.nicmar.ac.in

Received: 30 November 2025 | Revised: 28 December 2025 | Accepted: 9 January 2026

 DOI: https://doi.org/10.48084/etasr.16619

ABSTRACT

This study assesses the electrochemical compatibility of steel reinforcement with molten sulfur in Sulfur-Infiltrated Concrete (SIC) through integrated electrochemical and compositional analyses. Twelve cylindrical concrete specimens (100 mm × 200 mm) with 10-mm-diameter Fe550D steel reinforcement embedded in them were prepared: six with sulfur infiltration and six without. Half-cell potential measurements were conducted on triplicate specimens from each series at 1-day and 28-day curing ages according to ASTM C876-15. These measurements were complemented by Scanning Electron Microscopy and Energy Dispersive X-ray spectroscopy (SEM-EDX) characterization at 28 days. The results show that sulphur infiltration does not adversely affect the electrochemical state of embedded steel reinforcement. SIC specimens exhibited corrosion potentials of −181 mV (1-day) and −211 mV (28-day) versus −193 mV and −237 mV for conventional concrete. Both specimen types remained within the low corrosion probability range (more positive than −350 mV versus CSE) according to ASTM C876 criteria, confirming that exposure to molten sulphur at 140°C does not initiate corrosion. SEM imaging revealed a modified pore structure with a sulfur coating on cement particles. EDX analysis confirmed a fivefold higher sulfur content in SIC (2.6 wt%) than in conventional concrete (0.5 wt%). These findings establish the electrochemical compatibility of sulfur infiltration with steel reinforcement and validate that the SIC process does not compromise steel passivity, making it suitable for reinforced concrete precast applications.

Keywords-corrosion assessment; steel reinforcement; sulphur infiltrated concrete; half-cell potential; SEM-EDX; electrochemical compatibility

I. INTRODUCTION

Corrosion of steel reinforcement causes failure of reinforced concrete structures, leading to a reduced lifespan, loss of structural capacity, and significant economic impacts. Corrosion is triggered by the breakdown of the passive oxide layer on steel due to carbonation or chloride ingress, affected by concrete permeability, moisture availability, oxygen diffusion, and environmental exposure conditions [1-3]. SIC is a composite material produced by infiltrating molten sulfur into the pore structure of hardened Portland cement concrete [4]. Authors in [5-7] showed that sulfur infiltration significantly reduces porosity and enhances the compressive strength and chemical resistance of concrete by filling capillary voids within the cement matrix. The process typically involves heating sulfur above its melting point and allowing it to penetrate the concrete matrix under controlled thermal conditions. While the material-level benefits of SIC are well documented, concerns have been raised about the potential effects of exposing embedded steel reinforcement to elevated temperatures and molten sulfur during infiltration on steel passivity and interfacial stability [8, 9]. Most existing research on sulfur-based concretes has focused on the mechanical performance, microstructural refinement, and durability enhancement of the concrete matrix itself. Limited attention has been given to the

electrochemical behavior of embedded steel reinforcement [9–11]. The potential interaction between molten sulfur and steel surfaces, coupled with thermal stresses induced during heating and cooling cycles, necessitates a systematic evaluation of steel-sulfur compatibility. The absence of a standardized electrochemical evaluation method based on established corrosion assessment techniques has created a significant knowledge gap regarding the feasibility of sulfur infiltration in reinforced concrete systems [10, 12]. This study presents the first systematic electrochemical evaluation of steel-sulfur compatibility, using ASTM C876-15 half-cell potential testing alongside microstructural characterization, examining the behavior of steel reinforcement during and after sulfur infiltration. Thus, it establishes the suitability of SIC for reinforced and precast structural applications. This study tries to evaluate the effect of 4-h sulfur infiltration at 140°C on the corrosion potential and electrochemical characteristics of embedded steel reinforcement by taking half-cell potential measurements at 1-day and 28-day curing periods. In addition, the microstructural changes and sulfur distribution in the concrete matrix using SEM-EDX characterization to validate the electrochemical compatibility of sulfur infiltration with steel reinforcement for reinforced concrete applications, were analyzed.

II. MATERIALS AND METHOD

A. Materials

Grade 53 Ordinary Portland Cement (OPC), which conforms to IS 12269:2013, was used, with a specific gravity of 3.15 and a fineness of 320 m²/kg. Manufactured sand (M-sand) that met Zone II grading requirements, as well as crushed stone coarse aggregates (10 mm and 20 mm) that conformed to IS 383:2016, were also used. All aggregates were thoroughly washed to remove dust and deleterious materials. High-strength, deformed steel bars (Fe 550D grade; 10 mm in diameter) that conformed to IS 1786:2008 were used for reinforcement. Commercial-grade elemental sulfur (with >99% purity) was utilized for infiltration. These materials represent the standard specifications for precast concrete construction in India, ensuring the practical relevance of the findings. Tap water that met the requirements of IS 456:2000 was used for mixing and curing.

B. Mix Design and Specimen Preparation

The concrete mix design followed the guidelines of IS 10262:2019, and the proportions are presented in Table I. The high water-to-cement ratio of 0.70 was intentionally chosen to allow for sufficient porosity and promote effective sulfur infiltration.

TABLE I. CONCRETE MIX PROPORTIONS

Materials	Quantity (kg/m^3)
Cement (OPC 53 Grade)	300
Fine aggregate (M-sand)	847
Coarse aggregate (20 mm)	652
Coarse aggregate (10 mm)	377
Water	210
Water-cement ratio (w/c)	0.70
Aggregate-cement ratio (a/c)	4.08

Cylindrical specimens with a diameter of 100 mm and a height of 200 mm were cast according to the specifications of IS 516:2021, with centrally embedded steel bars with a diameter of 10 mm, as shown in Figure 1 (a). Fresh concrete was placed in three layers and properly compacted using a 16 mm tamping rod. The specimens were demolded after 24 h, as depicted in Figure 1 (b), and divided into two groups. Group 1 was tested at one day, and Group 2 was cured in water at 27 ± 2°C for 28 days.

(a) (b)

Fig. 1. (a) Casting of concrete specimens, (b) specimens after demoulding.

C. Sulphur Infiltration Process

As presented in Figure 2, the sulfur infiltration process was conducted in four stages. The designated specimens underwent oven drying at 105-110°C for 24 h to remove moisture. Then, commercial sulfur was melted at 140 ± 5°C in a stainless-steel heating chamber. The dried specimens were fully immersed in the molten sulfur at 140°C for 4 h under normal atmospheric pressure to allow for capillary penetration into the pore network. After infiltration, the specimens were removed and cooled gradually to an ambient temperature of 25 ± 3°C over 2-3 h to allow the sulfur to solidify within the concrete matrix. The infiltration temperature and duration were selected based on preliminary trials and a literature review to ensure adequate sulfur penetration while avoiding thermal damage to the cement matrix and embedded steel reinforcement; however, these values may vary depending on the sample size.

D. Half-Cell Potential Testing

Half-cell potential measurements were conducted according to ASTM C876-15 using a Giatec device, as portrayed in Figure 3, with a copper-Copper Sulfate reference electrode (CSE). The concrete surfaces were lightly moistened with a damp sponge to enhance ionic conductivity. The reference electrode was placed in multiple locations (at least 5 per specimen) on the concrete surface. The electrode was stabilized for 30 s-60 s before each reading was recorded. Measurements were performed at an ambient laboratory temperature of 25 ± 3 °C and a relative humidity of 60 ± 10%. According to ASTM C876-15 interpretation criteria, potentials more positive than -200 millivolts (mV) (CSE) indicate low corrosion probability; potentials between -200 and -350 mV indicate intermediate risk; and potentials more negative than -350 mV indicate high corrosion probability.

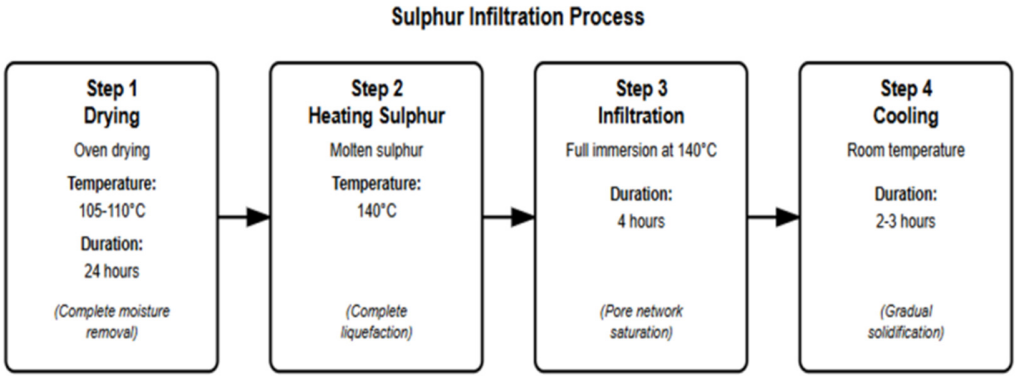

Fig. 2. Schematic diagram of the sulphur infiltration process showing the four-step procedure.

Fig. 3. Half-cell potential measurement on concrete specimen.

E. Microstructural Characterization

SEM and Energy-Dispersive Spectroscopy (EDS) were performed on selected specimens to examine the morphology of the concrete matrix and the distribution of sulfur. The concrete samples were crushed into a powder, oven-dried at 60°C for 24 h, mounted on aluminum stubs, and sputter-coated with gold. SEM imaging was conducted at 500× and 800× magnifications. EDS elemental analysis was performed to identify and quantify the distribution of sulfur, calcium, silicon, and aluminum within the concrete matrix.

F. Testing Program and Statistical Analysis

A total of 12 cylindrical specimens were prepared and tested: 6 specimens at 1 day (3 NCC and 3 SIC) and 6 specimens at 28 days (3 NCC and 3 SIC). All half-cell potential measurements were performed in triplicate (n = 3) and are presented as the mean ± standard deviation. The statistical significance between the SIC and NCC specimens was evaluated using a student's t-test with a significance level of $p < 0.05$.

III. RESULTS AND DISCUSSION

A. Half-Cell Potential Measurements at 1-Day Curing

As displayed in Table II and Figure 4, notable differences were revealed in the half-cell potential measurements conducted on specimens after 1 day of curing between SIC and NCC.

TABLE II. HALF-CELL POTENTIAL VALUES AT 1-DAY CURING

Specimen type	Sample 1 (mV)	Sample 2 (mV)	Sample 3 (mV)	Average (mV)
SIC	-186	-176	-181	-181 ± 5.0
NCC	-194	-187	-198	-193 ± 5.6

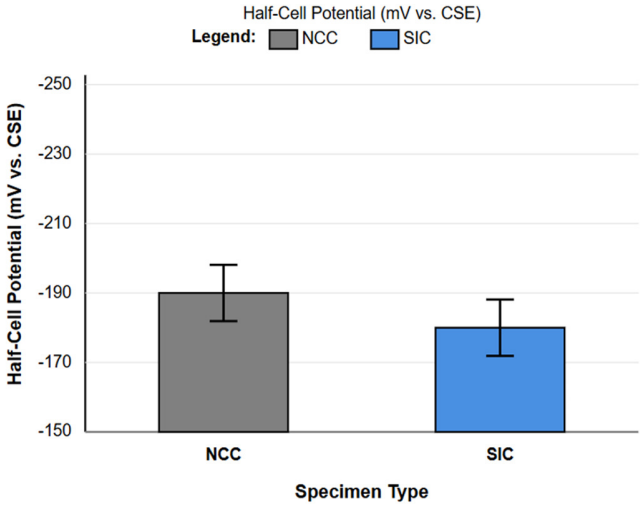

Fig. 4. Comparison of half-cell potential values at 1 day of curing for NCC and SIC. Error bars represent standard deviation (n = 3). SIC specimens exhibit more positive potentials (-181 ± 5.0 mV) compared to NCC specimens (-193 ± 5.6 mV). The difference of 12 mV is statistically significant ($p < 0.05$).

After 1 day of curing, SIC specimens exhibited less negative half-cell potentials than NCC specimens. The average potential for SIC was −181 ± 5.0 mV (CSE), compared to −193 ± 5.6 mV for NCC—a difference of 12 mV. A student's t-test confirmed that this difference was statistically significant ($p < 0.05$), indicating that SIC had better early-age electrochemical

protection. According to ASTM C876-15, both mixes fall within the low-corrosion-probability range (>−200mV). However, SIC's comparatively more positive values indicate enhanced protection, likely due to sulfur infiltration reducing pore connectivity and improving the concrete's early-age density.

B. Half-Cell Potential Measurements at 28-Day Curing

As shown in Table III and Figure 5, the half-cell potential measurements conducted after 28 days of curing revealed more significant differences between SIC and NCC specimens than the 1-day results.

TABLE III. HALF-CELL POTENTIAL VALUES AT 28-DAY CURING

Specimen type	Sample 1 (mV)	Sample 2 (mV)	Sample 3 (mV)	Average (mV)
SIC	-224	-200	-211	-211 ± 12.0
NCC	-238	-230	-243	-237 ± 6.5

After 28 days of curing, the average half-cell potential of SIC specimens was -211 ± 12.0 mV (CSE), while the average half-cell potential of NCC specimens was significantly more negative at -237 ± 6.5 mV (CSE), representing a difference of 26 mV. Statistical analysis confirmed that this difference is highly significant ($p < 0.01$), demonstrating that the protective effect of sulfur infiltration becomes more evident with age. According to ASTM C876-15 standards, both specimen types remained within the low to intermediate corrosion probability range. Temporal analysis reveals important trends in the electrochemical behavior of embedded steel. For NCC specimens, the average potential shifted from -193 mV at 1 day to -237 mV at 28 days, representing a 44 mV increase in negativity. In contrast, SIC specimens exhibited a smaller shift, from -181 mV to -211 mV, indicating an increase of only 30 mV. This differential behavior suggests that sulfur infiltration becomes increasingly effective as the concrete matures.

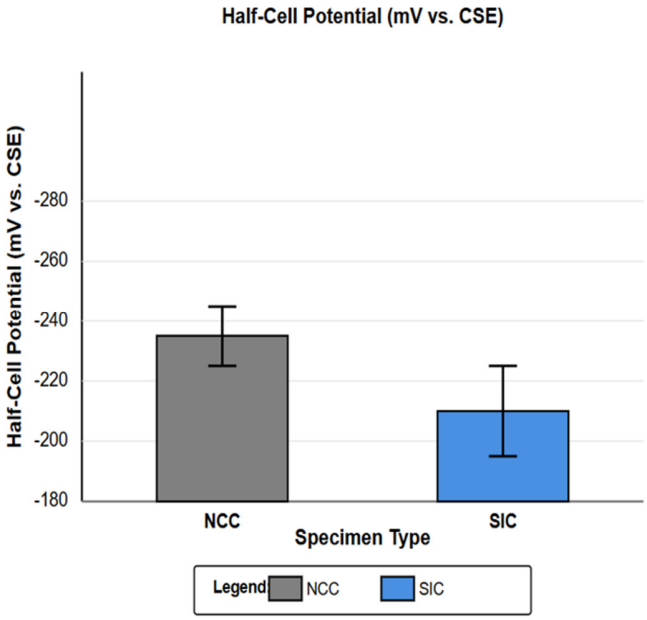

Fig. 5. Comparison of half-cell potential values at 28 days of curing for NCC and SIC. Error bars represent standard deviation (n = 3). SIC specimens show -211 ± 12.0 mV compared to NCC specimens at -237 ± 6.5 mV, representing a 26 mV improvement ($p < 0.01$), more than double the 1-day differential.

C. Statistical Analysis and Comparative Evaluation

The statistical analysis shows that sulfur infiltration does not negatively impact the corrosion state of embedded steel reinforcement. Half-cell potential measurements at two curing ages confirm the electrochemical compatibility between the steel and the sulfur-infiltrated matrix, as depicted in Table IV.

TABLE IV. COMPARATIVE ANALYSIS OF HALF-CELL POTENTIALS

Parameter	1-day curing	28-day curing
SIC average (mV)	-181 ± 5.0	-211 ± 12.0
NCC average (mV)	-193 ± 5.6	-237 ± 6.5
Difference (mV)	12	26
Improvement (%)	6.2	11.0
Statistical significance	$p < 0.05$	$p < 0.01$

Statistical analysis confirms that SIC and NCC specimens maintained half-cell potentials within the acceptable range according to the ASTM C876-15 criterion at both curing ages. All specimens remained in the low-to-intermediate corrosion probability range (more positive than -350 mV), indicating passive steel conditions. The consistently acceptable values in the SIC specimens show that 4 h of exposure to molten sulfur at 140°C does not initiate corrosion or damage the passive film on the steel reinforcement. Both specimen types exhibited similar temporal changes in half-cell potentials, characteristic of normal concrete maturation. These results validate the electrochemical compatibility of sulfur infiltration with embedded steel reinforcement. The more positive half-cell potentials in the SIC specimens suggest that sulfur infiltration enhances the electrochemical stability of the steel-concrete system by reducing ionic conductivity and limiting electrochemical activity at the steel surface.

D. Microstructural Analysis

1) Scanning Electron Microscopy Analysis

Concrete samples for SEM- EDX analysis were extracted from the mid-height region of cube specimens (away from steel reinforcement to avoid interface effects) to characterize the bulk concrete matrix. Sample sets were selected from NCC and SIC specimens to ensure a comparative analysis of microstructural changes due to sulfur infiltration. Examination by scanning electron microscopy at 800× and 1000× magnifications revealed distinct microstructural differences between the two types of specimens. The NCC specimens exhibited a heterogeneous microstructure with clearly visible porous regions and distinct particle boundaries, as shown in Figures 6 and 7.

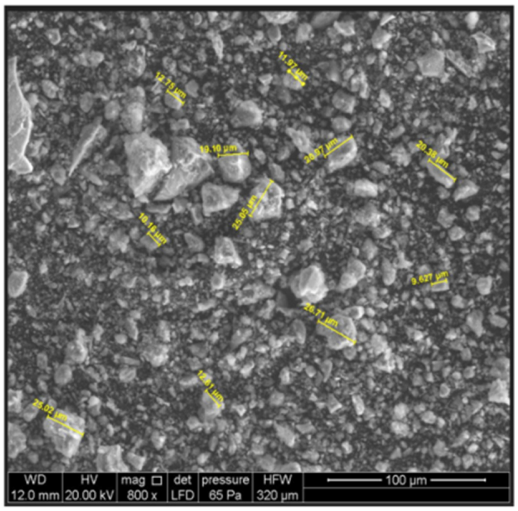

Fig. 6. SEM image of NCC specimen at 800× magnification showing porous microstructure with distinct particle boundaries.

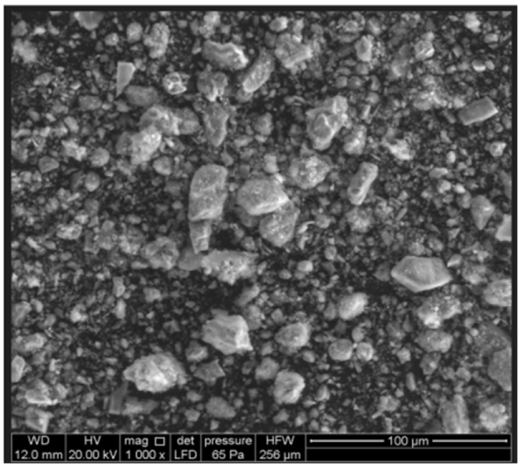

Fig. 7. SEM image of NCC specimen at 1000× magnification showing individual cement particles and visible voids.

The cement matrix showed typical hydration products with particle sizes ranging from approximately 9 µm to 26 µm. Individual cement particles and aggregates were distinguishable, with visible gaps and voids indicating an open pore structure, which is characteristic of conventional concrete. In contrast, SIC specimens displayed a significantly more compact microstructure with reduced porosity, as illustrated in Figures 8 and 9. Their particle sizes ranged from 27 µm to 63 µm, and they showed improved particle packing and denser matrix formation. The cement particles appeared more closely bound together, indicating effective sulfur infiltration into the pore network. Microstructural examination confirms that sulfur penetrated the capillary pores and voids, creating a denser concrete matrix than conventional concrete.

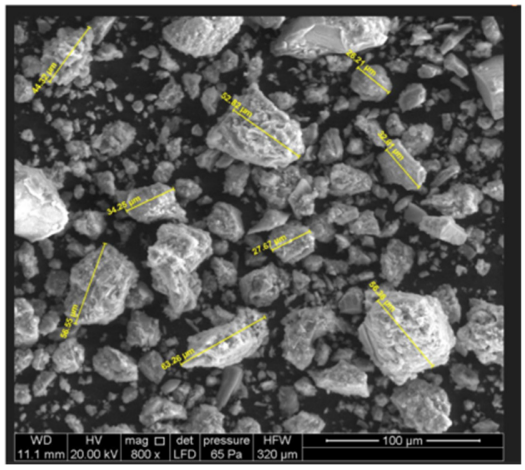

Fig. 8. SEM image of SIC specimen at 800× magnification showing denser microstructure with improved particle packing.

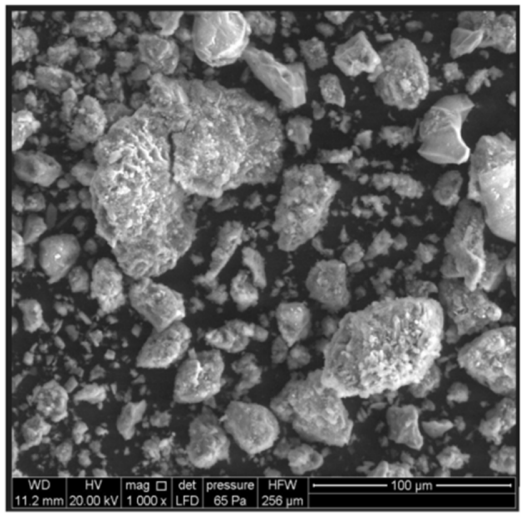

Fig. 9. SEM image of SIC specimen at 1000× magnification showing compact matrix with reduced porosity.

2) Energy Dispersive X-Ray Spectroscopy (EDX) Analysis

X-ray EDS confirmed the presence and quantified the number of key elements within the concrete matrix for both specimen types. The elemental composition analysis is displayed in Table V, with the EDS analysis revealing a significant difference in sulfur content between the two specimen types. NCC specimens exhibited a minimal sulfur content of 0.3 wt%, likely due to trace amounts present in the cement or aggregates. In contrast, SIC specimens exhibited a substantially higher sulfur content of 2.3 wt%, confirming the successful infiltration of sulfur into the concrete matrix. The presence of 2.3 wt% sulfur in SIC specimens confirms the infiltration process's effectiveness in introducing sulfur into the pore network. The elemental compositions of NCC and SIC were largely comparable, with typical cement constituents, such as calcium, silicon, and aluminum, present in both. Minor variations in elemental percentages are attributed to the heterogeneous nature of concrete and the localized EDS sampling areas.

The iron content was low in both specimens (3.7 wt% in NCC and 4.3 wt% in SIC), indicating that the steel reinforcement did not significantly impact the surface elemental composition of the powdered samples. These results suggest that EDS measurements primarily reflect the concrete matrix rather than the embedded steel.

TABLE V. EDS ELEMENTAL COMPOSITION (WEIGHT %)

Element	NCC	SIC
Carbon (C)	12.4	14.8
Oxygen (O)	53.0	51.6
Sodium (Na)	2.4	2.8
Magnesium (Mg)	0.7	1.2
Aluminum (Al)	5.1	6.5
Silicon (Si)	12.8	11.7
Sulphur (S)	0.3	2.3
Potassium (K)	0.2	0.3
Calcium (Ca)	9.4	4.5
Iron (Fe)	3.7	4.3

E. Correlation between Microstructure and Electrochemical Behavior

The microstructural analysis corroborates the electrochemical findings from half-cell potential measurements. The protective mechanism operates through sulfur-induced pore refinement, whereby infiltrated sulfur fills capillary pores (2.3 wt% in SIC versus 0.3 wt% in NCC). This creates a denser, less permeable matrix that restricts the transport of oxygen and moisture to the steel surface, preserving the protective passive film. The denser microstructure observed in SIC specimens, combined with the confirmed presence of sulfur within the pore network (2.3 wt%), demonstrates that sulfur infiltration successfully modifies the concrete matrix without creating conditions that are detrimental to steel reinforcement. The passive state of the steel in the SIC specimens, as evidenced by the acceptable half-cell potential values, confirms the electrochemical compatibility of the sulfur-modified matrix with reinforced concrete applications.

IV. CONCLUSIONS

Based on the experimental analysis of steel-sulfur compatibility in Sulfur-Infiltrated Concrete (SIC) using half-cell potential testing and microstructural analysis, the following conclusions were drawn:

- The molten sulfur infiltration process at 140°C for 4 h did not adversely affect the corrosion state of embedded steel reinforcement. Both conventional concrete and SIC specimens exhibited half-cell potential values within the passive range throughout the testing period, confirming that sulfur infiltration does not initiate corrosion processes.
- All specimens remained within the low-to-intermediate corrosion probability range (more positive than -350 mV), according to ASTM C876-15 criteria, at both the 1-day and 28-day curing ages. SIC specimens showed average potentials of -181 mV at 1 day and -211 mV at 28 days, while conventional concrete exhibited -193 mV at 1 day and -237 mV at 28 days, indicating stable passive conditions in both cases.
- Microstructural analysis using Scanning Electron Microscopy (SEM) revealed that SIC specimens exhibited a denser microstructure than conventional concrete. Sulfur effectively filled the capillary pores and voids. EDS analysis confirmed successful sulfur infiltration, with SIC specimens showing a sulfur content of 2.3 wt%, compared to 0.3 wt% in conventional concrete.
- Both SIC and conventional concrete specimens exhibited similar temporal changes in half-cell potentials, confirming that sulfur infiltration does not affect the natural electrochemical equilibrium between steel and concrete.
- These findings establish that sulfur infiltration is electrochemically compatible with embedded steel reinforcement, confirming the SIC technology for precast reinforced concrete applications, particularly in aggressive environments where durability and structural integrity are critical.

This is the first systematic electrochemical assessment to validate steel-sulfur compatibility in SIC, expanding on existing studies of mechanical properties. Future research should focus on evaluating long-term corrosion behavior through extended monitoring periods and accelerated exposure testing under simulated aggressive environmental conditions. To validate the practical applicability of this technology for infrastructure applications, performance assessment of full-scale reinforced SIC structural elements under actual service conditions is proposed. Additionally, long-term performance monitoring (2-5 years) of SIC structures in actual marine and industrial environments, with periodic half-cell potential measurements and visual inspections, can be carried out to validate field durability.

REFERENCES

[1] A. Poursaee, *Corrosion of Steel in Concrete Structures*, 2nd ed. Cambridge, UK: Woodhead Publishing, 2016.

[2] G. Song and A. Shayan, "Corrosion of steel in concrete: causes, detection and prediction," *Australian Journal of Civil Engineering*, vol. 16, no. 1, pp. 15–23, July 1998.

[3] M. Stefanoni, U. Angst, and B. Elsener, "Corrosion rate of carbon steel in carbonated concrete – A critical review," *Cement and Concrete Research*, vol. 103, pp. 35–48, Jan. 2018, https://doi.org/10.1016/j.cemconres.2017.10.007.

[4] A. M. Ali, L. F. Hussein, and R. M. Khudada, "The Behavior of Corroded Reinforced Concrete Beams under External Loads: A Literature Review," *Engineering, Technology & Applied Science Research*, vol. 15, no. 5, pp. 27872–27876, Oct. 2025, https://doi.org/10.48084/etasr.12152.

[5] N. Thaulow, "Sulphur-impregnated concrete, SIC.," *Cement and Concrete Research*, vol. 4, no. 2, pp. 269–277, Mar. 1974, https://doi.org/10.1016/0008-8846(74)90138-0.

[6] "Sulphur Concrete and Sulphur Infiltrated Concrete: Properties, Applications, and Limitations," Canada Centre for Mineral and Energy Technology, Minerals Research Program, Mineral Sciences Laboratories, Energy, Mines and Resources Canada, Ottawa, ON, Canada, Technical 79–28, 1979.

[7] V. Malhotra, "Development of Sulfer-Infiltrated High-Strength Concrete," *ACI Journal Proceedings*, vol. 72, no. 9, 1975, https://doi.org/10.14359/11150.

[8] M. Hashami, Y. Ongarbayev, Y. Tileuberdi, Y. Imanbayev, A. Zhambolova, and Y. Kanzharkan, "Technological Progress in Sulfur-Based Construction Materials: The Role of Modified Sulfur Cake in Concrete and Bitumen," *Applied Sciences*, vol. 15, no. 16, p. 8790, Jan. 2025, https://doi.org/10.3390/app15168790.

[9] R. Fediuk *et al.*, "A Critical Review on the Properties and Applications of Sulfur-Based Concrete," *Materials*, vol. 13, no. 21, Jan. 2020, Art. no. 4712, https://doi.org/10.3390/ma13214712.

[10] *C876-22b Standard Test Method for Corrosion Potentials of Uncoated Reinforcing Steel in Concrete*. West Conshohocken, PA, USA: ASTM International, 2015.

[11] G. H. Pathak and S. Charhate, "Experimental investigation on mechanical and microstructural properties of sulphur-infiltrated concrete (SIC)," *Discover Civil Engineering*, vol. 2, no. 1, Nov. 2025, Art. no. 204, https://doi.org/10.1007/s44290-025-00367-w.

[12] L. Bertolini, B. Elsener, P. Pedeferri, E. Redaelli, and R. B. Polder, *Corrosion of Steel in Concrete: Prevention, Diagnosis, Repair*. Weinheim, Germany: John Wiley & Sons, 2013.